Supplementary Material (ESI) for Chemical Communications
This journal is (c) The Royal Society of Chemistry 2009

Caterina Fraschetti, Marco Pierini, Claudio Villani, Francesco Gasparrini, Stefano Levi Mortera, and Maurizio Speranza**

Towards Enzyme-like Enantioselectivity in the Gas Phase: Conformational Control of Selectivity in Chiral Macrocyclic Dimers.

SUPPORTING INFORMATION

FT-ICR Experiments. Kinetic experiments were performed at room temperature in an APEX 47e FT-ICR mass spectrometer equipped with an ESI source (Bruker Spectrospin) and a resonance cell ("infinity cell") situated between the poles of a superconducting magnet (4.7 T). Stock solutions of the macrocycle $M^{R/S}$ ($1x10^{-5}$ M) in CH_3OH, containing an equimolar amount of A^S, were electrosprayed through a heated capillary (130 °C) into the external source of the FT-ICR mass spectrometer. The resulting ions were transferred into the resonance cell by a system of potentials and lenses and quenched by collisions with methane pulsed into the cell through a magnetic valve. Abundant signals, corresponding to the natural isotopomers of the proton-bound complexes $[(M^{R/S})_2 \bullet H \bullet A^S]^+$, were monitored and isolated by broad-band ejection of the accompanying ions. The $[(M^{R/S})_2 \bullet H \bullet A^S]^+$ complexes were then allowed to react with the chiral amine B present in the cell at a fixed pressure whose value ranges from $2.6x10^{-7}$ to $2.9x10^{-7}$ mbar depending upon its reactivity (Figures S0-S4).

Figure S0. Typical FT-ICR mass spectra showing the time-dependent abundances of the $[(M^S)_2•H•A^S]^+$ reactant and its product $[(M^S)_2•H•B^R]^+$ by reaction with B^R ($P = 2.8x10^{-7}$ mbar)

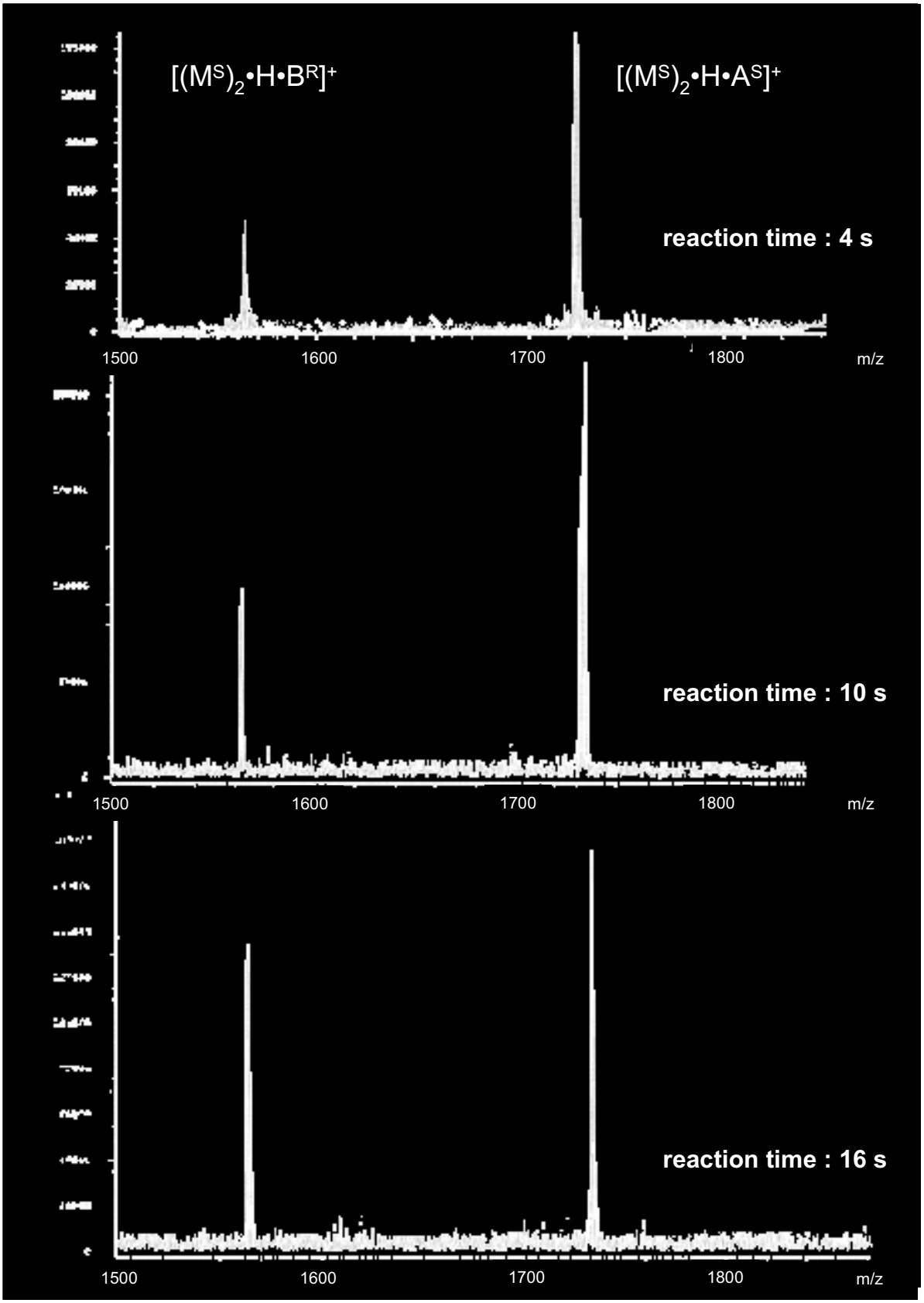

Kinetic Results

Kinetic plots (Figures S1-S4) of the gas-phase reaction between $[(M^{R/S})_2 \bullet H \bullet A^S]^+$ and $B^{R/S}$.

Figure S1. Kinetic plots for the gas-phase reaction of the $[(M^R)_2 \cdot H \cdot A^S]^+$ complex with B^R ($P = 2.9 \times 10^{-7}$ mbar).

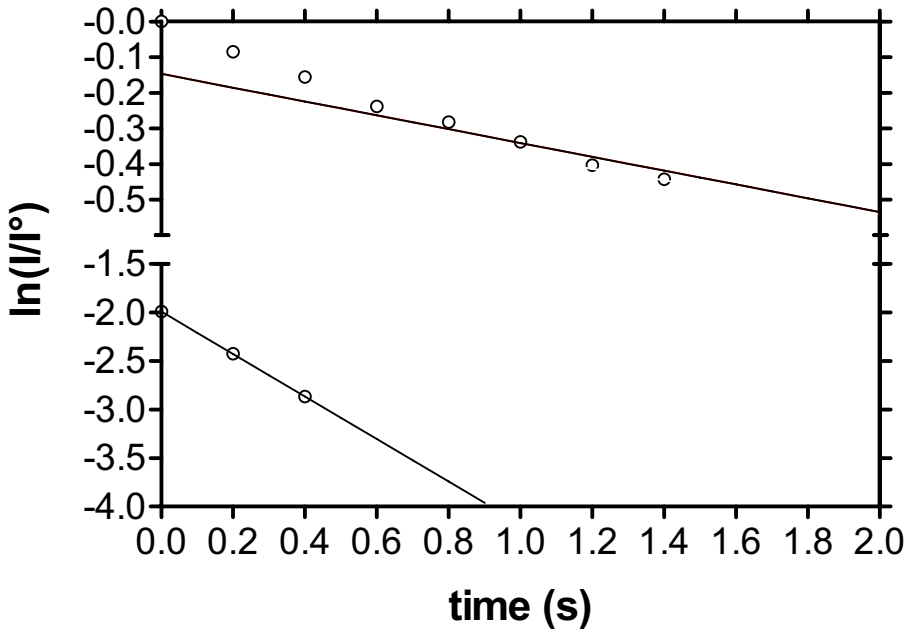

Figure S2. Kinetic plots for the gas-phase reaction of the $[(M^S)_2 \cdot H \cdot A^S]^+$ complex with B^R ($P = 2.8 \times 10^{-7}$ mbar).

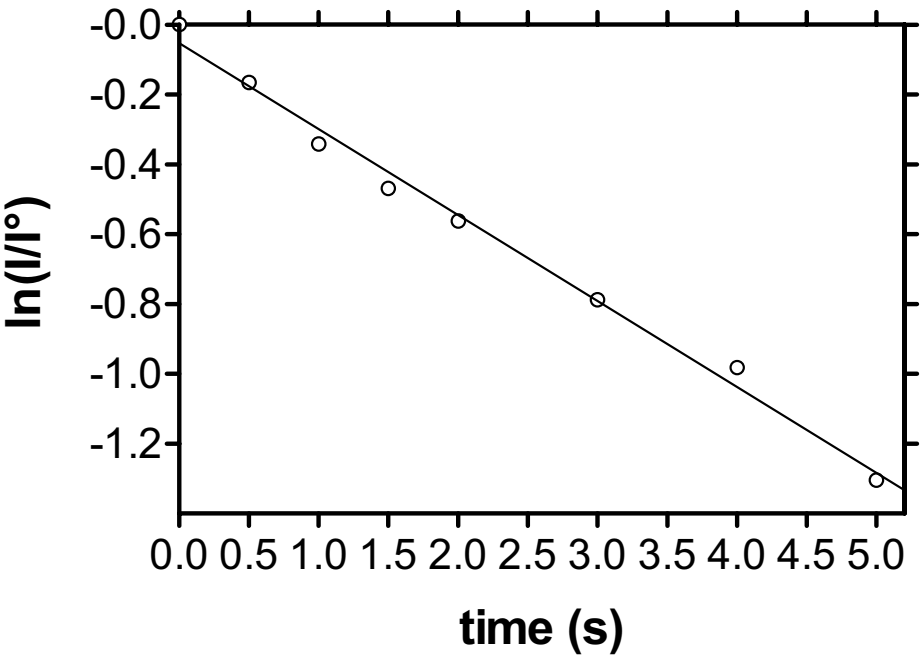

Figure S3. Kinetic plots for the gas-phase reaction of the $[(M^R)_2 \cdot H \cdot A^S]^+$ complex with B^S ($P = 2.6 \times 10^{-7}$ mbar).

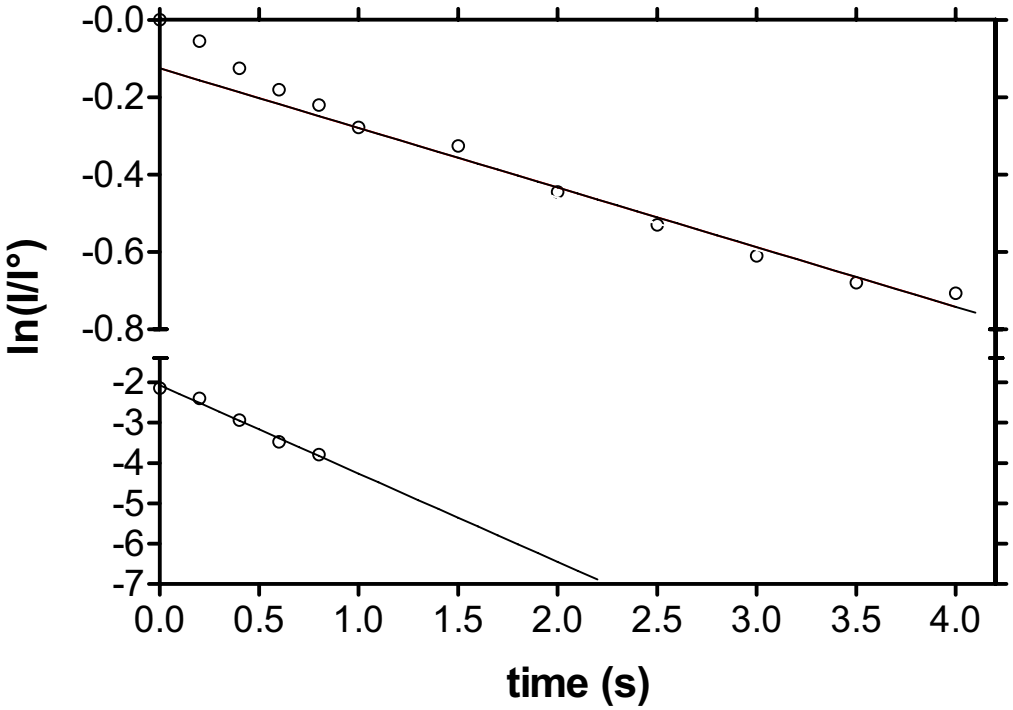

Figure S4 Kinetic plots for the gas-phase reaction of the $[(M^S)_2 \cdot H \cdot A^S]^+$ complex with B^S ($P = 2.6 \times 10^{-7}$ mbar).

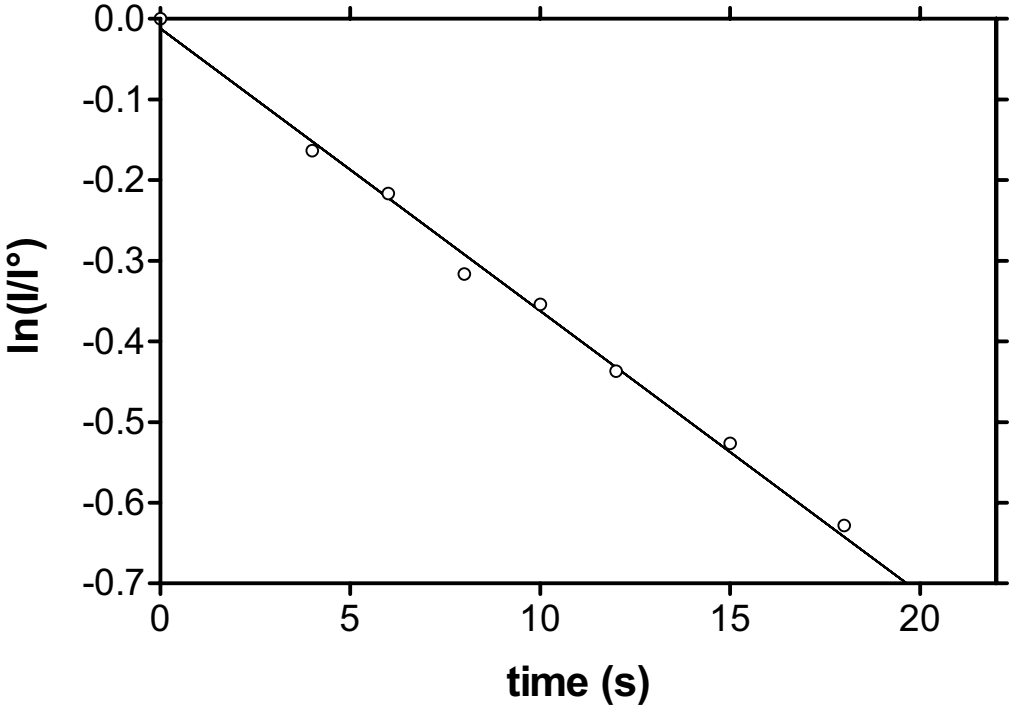

Computational Details. To obtain a realistic simulation of the diastereomeric $[(M^R)_2•H•A^{R/S}]^+$ complexes adducts, an original procedure has been adopted which has been recently tested in simpler complexes (ref. [1S]). Such an approach involves the initial generation of the two-body $[M^R•H•A^{R/S}]^+$ diastereoisomers obtained by docking one to each other the more representative conformations of the tetra-amidic host M^R against those of the guest $A^{R/S}$. The achieved most populated two-body $[M^R•H•A^{R/S}]^+$ adducts, clustered in a limited number of members, have been collected in two (homo and heterochiral) ensembles. As mentioned before, the host molecule frequently assumes in these ensembles the *ax-ax* disposition by induced fit on complexation with the host (ref. [2S]). Then, a further docking procedure between the members of the two-body $[M^R•H•A^{R/S}]^+$ complexes and the most representative conformations of the host M^R, gave rise to two final populations of three-body $[(M^R)_2•H•A^{R/S}]^+$ supramolecules. Accordingly, the calculated structures of both the homo- $[(M^R)_2•H•A^R]^+$ and the heterochiral $[(M^R)_2•H•A^S]^+$ aggregates can in turn be conveniently clustered, within a 3 kcal mol^{-1} energy window, in two ensembles denoted as **I** and **II**. The most representative members of these ensembles are reported in Figure 1 of the main text.

All calculations were performed with software packages running on a PC equipped with Intel Pentium 4. Simulations *in vacuo* of the diastereomeric $[(M^R)_2•H•A^{R/S}]^+$ complexes were carried out by docking the macrocycles M^R and the protonated $A^{R/S}$ according to the procedure described above. The three-body adducts $[(M^R)_2•H•A^R]^+$ and $[(M^R)_2•H•A^S]^+$ were generated by docking one to each other the more representative $[M^R•H•A^R]^+$ and $[M^R•H•A^S]^+$ structures (two geometries each with the host in *ax-ax* (Boltzmann Population (BP): 87% (A^R); 79% (A^S)) and *eq-eq* conformation (BP: 13% (A^R); 21% (A^S)) against the most significant geometries of the host M^R (three conformations representative of the *eq-eq* (BP: 98.4%), *ax-ax* (BP: 1.5%), and *ax-eq* (BP: 0.1%)). Dockings experiments were carried out in two steps: 1) multiconformational rigid docking performed on each couple of host and guest structures using the MolInE program (refs. 3S-5S). The host–guest approach options set were: 52 directions of translation and 272 relative orientations of guest to host for each couple of host–guest geometries; 2) selection performed on the ensemble of adducts obtained in the first step, using energetic and geometric criteria. The geometry of the so achieved complexes was then optimized by full relaxing their structure using the Batchmin program with the following options set: MM2* Force Field, PR conjugate gradient minimization. All the conformer ensembles were analyzed by C.A.T. program to exclude twin molecules, make energetic clusters and perform calculations of Boltzmann populations.

References.

[1S] C. Fraschetti, M. Pierini, C. Villani, F. Gasparrini, A. Filippi, M. Speranza : *Collect. Czech. Chem. Commun.* **2009**, *74*, 275-297.

[2S] F. Gasparrini, M. Pierini, C. Villani, A. Filippi, M. Speranza : *J. Am. Chem. Soc.* **2008**, *130*, 522-534.

[3S] Alcaro S., Gasparrini F., Incani O., Mecucci S., Misiti D., Pierini M., Villani C.: *J. Comput. Chem*. **2000**, *21*, 515-530.

[4S] Angelini G., Cerichelli G., Cerritelli S., Pierini M., Siani G., Villani C.: *J. Comput.-Aided Mol. Des*. **2005**, *19*, 259-269.

[5S] Alcaro S., Gasparrini F., Incani O., Caglioti L., Pierini M., Villani C.: *J. Comput. Chem*. **2007**, *28*, 1119-1128.

Figures S4 and S5

Structures of complexes formed by the tetra-amidic macrocycle M^R host and the guest $A^{R/S}$ *(It should be noted that we found more convenient to simulate the experimental $[(M^{R/S})_2 \bullet H \bullet A^S]^+$ systems using a fixed configuration for the host (M^R) and the two enantiomers of the guest ($A^{R/S}$). For the sake of clarity, in the main text, we always denoted the homochiral adduct as $[(M^S)_2 \bullet H \bullet A^S]^+$, even though calculations are on $[(M^R)_2 \bullet H \bullet A^R]^+$. As far as the isolated homochiral $[(M)_2 \bullet H \bullet A]^+$ complexes are considered, these configurational inversions do not produce any consequences).*

Figure S5 Hydrogen bonds within the most stable geometries of the homochiral $[(M^R)_2 \bullet H \bullet A^R]^+$ and heterochiral $[(M^R)_2 \bullet H \bullet A^S]^+$ complexes. For sake of clarity all structures are plotted with hided hydrogen atoms, with the exception of those ones bonded to nitrogen atoms.

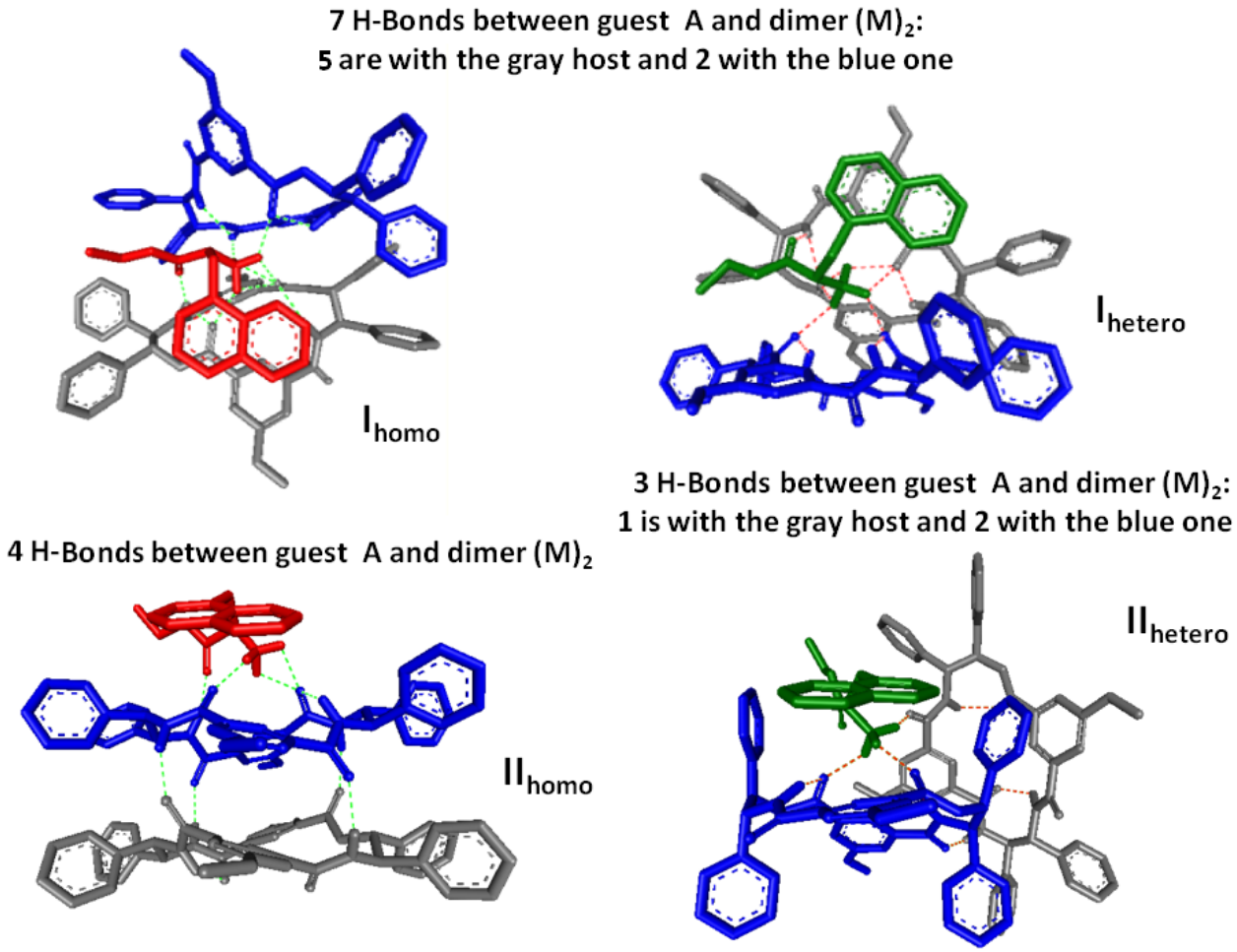

Figure S6. Structural relationship between three-body $\mathbf{II}_{homo}$ and its two-body homochiral $[M^{R}{\bullet}H{\bullet}A^{R}]^{+}_{fast}$ counterpart.